Journal of Pharmaceutical Sciences 112 (2023) 243–249

Contents lists available at ScienceDirect

Journal of Pharmaceutical Sciences

journal homepage: www.jpharmsci.org

Pharmaceutics, Drug Delivery and Pharmaceutical Technology

Small Angle X-Ray Scattering Data Analysis and Theoretical Modelling for the Size and Shape Characterization of Drug Delivery Systems Based on Vitamin E TPGS Micelles

Liberato De Caro[a], Alessandra Del Giudice[b], Mickael Morin[c], Mathilde Reinle-Schmitt[c], Arnaud Grandeury[d,*], Fabia Gozzo[c,**], Cinzia Giannini[a,***]

[a] Istituto di Cristallografia, Consiglio Nazionale delle Ricerche, Via Amendola 122/O, 70125 Bari, Italy
[b] Sapienza University of Rome, Department of Chemistry, P.le Aldo Moro 5, 00185 Rome, Italy
[c] Excelsus Structural Solutions (Swiss) AG, PARK INNOVAARE deliveryLAB, 5234 Villigen, Switzerland
[d] Novartis Pharma AG, Technical Research and Development, Chemical and Pharmaceutical Profiling, Novartis Campus, Virchow 6.3.231, 4056 Basel, Switzerland

ARTICLE INFO

Article history:
Received 25 April 2022
Revised 29 September 2022
Accepted 29 September 2022
Available online 4 October 2022

Keywords:
Drug delivery systems
Vitamin E-TPGS
Surfactant
Active pharmaceutical ingredients
Eltrombopag
Small angle X-ray scattering
Micelles

ABSTRACT

We developed a simple two-dimensional/two-components theoretical model that describes the structure and functionality of a VitE-TPGS system of micelles assuming a hydrophobic inner core and an outer hydrated hydrophilic shell. We then conceptually applied the developed methodology to a simple system of VitE-TPGS micelles unloaded and loaded with an active pharmaceutical ingredient, eltrombopag, to verify if the model could reliably monitor the size change of the micelle upon loading. The fit of laboratory Small Angle X-Ray Scattering data against such model allows us to extract absolute values of the micelles size under a spherical shape hypothesis as well as the distribution within the system between components and level of hydration. The intensity scale of the SAXS experimental data needs to be normalized to a reference standard (pure water) to get absolute scattered intensities. The mathematical model which has been developed under a general hypothesis of ellipsoidal micelles, is applied to our experimental data under the simplified spherical assumption, which suitably fits our experimental data.

Introduction

The therapeutic properties of active pharmaceutical ingredients (API) can be preserved, enhanced and made safer by smart and creative drug formulations. Insoluble and poorly bioavailable drugs can significantly improve their bioavailability if administered via the intermediate of Drug Delivery Systems (DDS) acting either as solubility enhancer or vehicles that transport the API in the human body and administer it with the optimum dose and feeding regimen. In the recent years, pharmaceutical formulation has become an authentic engineering talent.

DDS are drug carriers whose dimension is in the nanoscale and of particular interest are lipid-based nanocarriers.[1] Interesting examples of lipid-based nanocarriers are nanovesicular carriers (e.g. niosomes, proniosomes, ethosomes, transferosomes, pharmacosomes, ufasomes, phytosomes, catanionic vesicles, and extracellular vesicles) capable of crossing the skin or the blood–brain-barrier and efficiently distribute the API they transport.[2] Because they behave as drug vessels that travel in the human body with a specific duty to absolve, their size, structure and morphology play a crucial role in their functionality. Characterizing their loaded and unloaded size and shape as a function of relevant human body parameters (e.g. pH or temperature), is therefore critical, especially if the characterization can be performed simulating the same condition of drug delivery, i.e. dispersed in a buffer which is often water. One of the most suitable techniques to perform such size, shape and morphology characterization is the Small Angle

Abbreviations: API, Active pharmaceutical ingredient; SAXS, Small angle X-ray scattering; Lab-SAXS, Laboratory small angle X-ray scattering; DDS, Drug delivery system; VitE-TPGS, vitamin E d-α-tocopherol polyethylene glycol 1000 succinate; FDA, Food and drug administration; PSC, Poorly soluble compound.

* Corresponding authors at: Novartis Pharma AG, Novartis Campus, Virchow 6.3.231, 4056 Basel, Switzerland.
** Corresponding authors at: Excelsus Structural Solutions (Swiss) AG, PARK INNOVAARE deliveryLAB, 5234 Villigen, Switzerland.
*** Corresponding authors at: Istituto di Cristallografia, Consiglio Nazionale delle Ricerche, Via Amendola 122/O, 70125 Bari, Italy.
E-mail addresses: arnaud.grandeury@novartis.com (A. Grandeury), fabia.gozzo@excelsus2S.com (F. Gozzo), cinzia.giannini@ic.cnr.it (C. Giannini).

https://doi.org/10.1016/j.xphs.2022.09.029
0022-3549/

X-ray Scattering (SAXS) technique[3] which dates back to 1950 with Guinier & Fournet[4] and to 1980 with Glatter & Kratky works.[5] The SAXS scattering data are collected in reciprocal space but to extract information in real space, a Fourier transform of the SAXS profile is needed to extract the corresponding Pair Distribution function PDF(r). PDF(r) allows us to estimate dimensions (maximum dimension (Dmax) and gyration radius (Rg)) and shape (globular, rod-like, multiple domains) of the scattering object, fundamental information for any ab-initio reconstruction of it. PDF(r) is also a quality check on the raw data,[6] and on sample preparation (no aggregation and interparticle interference). Small changes in the scattering curves are enhanced in the PDF(r) analysis, providing an accurate and sensible method for searching for tiny differences in the scattering sample.

The subject of our study is the interesting system of the lipid-based vitamin E D-α-tocopherol polyethylene glycol 1000 succinate (VitE-TPGS)[7] that enhances the bioavailability of poorly water-soluble drugs via these nanocarriers. VitE-TPGS forms stable micelles in water at low concentrations (critical micelle concentration of about 0.02%wt) and it is a safe pharmaceutic adjuvant already approved by the Food and Drug Administration (FDA) authorities. Not surprisingly, it is an attractive nanocarrier candidate.[8] This excipient is used as antioxidant, emulsifying agent, nonionic surfactant, solubilizing agent, suspending agent in tablet and capsule formulations. VitE-TPGS has a molecular structure of a typical amphiphile: the polar hydrophilic head of polyethylene glycol is linked to the nonpolar lipophilic tail of D-α-tocopherol and constitute the signature elements of molecules that form micelles in water. The chemical formula of VitE-TPGS is $C_{33}O_5H_{54}(CH_2\text{-}CH_2O)_n$ with n∼22-23. The value of n=22 leads to a 1kDa molecular weight for the PEG polymer.[8] For n∼22-23 (distribution 70/30) the average molecular weight is 1513 g/mol, with an expected diameter of ∼10-11 nm for the VitE-TPGS micelles when suitable monomer concentrations in water are selected.

When poorly aqueous soluble drugs are mixed with VitE-TPGS, stable micro-emulsions may be formed which eventually enhance the bioavailability of the drug, either by overcoming the poor solubility or by providing alternative transport mechanisms. In our study, the Poorly Soluble Compound (PSC) is an active pharmaceutical ingredient, so called eltrombopag. It is a thrombopoietin receptor agonist, which is used to treat low blood platelet counts in adults with chronic immune (idiopathic) thrombocytopenia. It has been approved by FDA in 2008.[9] The chemical structure of the compound is dominated by aromatic rings, which makes the compound hydrophobic. It also has a carboxylic group with an acidic pKa of 4.0 which helps improving its solubility in conditions close to neutral pH. The crystalline free acid is poorly soluble in aqueous media in acidic conditions and its solubility remains poor up to pH 6. The logD of the compound is 4.

The purpose of this study is to perform structural investigations of VitE-TPGS /PSC samples using laboratory Small Angle X-ray Scattering (lab-SAXS) enhanced by data expressed in absolute intensity units. VitE-TPGS/PSC samples were prepared with experimental parameters tuned on-purpose to observe the interaction between the PSC molecules and the VitE-TPGS carrier. Our goals were to i) develop an analytical method, based on the analysis of the PDF(r) function derived from lab-SAXS data; ii) quantify how many PSC molecules were incorporated in the VitE-TPGS micelles carriers, and where; iii) determine size and shape changes of the scattering objects.

Experimental Methods

Materials

Vitamin E-TPGS (chemical name 4-O-(2-Hydroxyethyl)-1-O-[2,5,7,8-tetramethyl-2-(4,8,12-trimethyltridecyl)-3,4-dihydrochromen-6yl] butanedioate), namely VitE-TPGS, is a synthetic product. It is available as a white to light-brown, waxy solid and is practically tasteless. Vitamin E-TPGS is stable at ambient room temperature for up to 4 years. It reacts with alkalis and acids. Aqueous solutions of vitamin E-TPGS are stable over a pH range of 4.5−7.5, and it is incompatible with strong acids and strong alkalis. The melting point of Vitamin E-TPGS is 37−41°C, therefore the storage conditions of the final drug product must be carefully evaluated. Vitamin E-TPGS meets the requirements of USP−NF. The safety of vitamin E polyethylene glycol succinate has been published, which includes a report showing no-observed-adverse-effect-level (NOAEL) in rats of 1000 mg/kg/day.[10]

The Poorly Soluble Compound (PCS) used in the study is eltrombopag as crystalline bis-(mono)ethanolamine salt (eltrombopag olamine, hereafter) and was provided by Novartis Pharma AG. The chemical purity used is higher than 99% and it is a crystalline solid. The crystal form corresponds to the powder diffraction data reported by Kaduk, J. *et al.*[11] with a density of 1.32 g/cm^3. The Differential Scanning Calorimetry (DSC) of eltrombopag bis-olamine exhibits several complex endothermic events above approximately 125°C, indicative of degradation and disproportionation.

Preparation of VitE-TPGS/PSC samples

VitE-TPGS/PSC samples, investigated by lab-SAXS, were prepared according to the protocol below:

a) *Solution of pH=6.8 (50 mM Phosphate buffer):* 682.7 mg of Potassium hydrogenphosphate (K_2HPO_4) and 90.4 mg of NaOH were added in a final volume of 100ml of H_2O Milli-Q. The solution was stirred until reaching a stabilized pH value of 6.8. The final value measured was pH=6.81. A stock solution of pH6.8 was prepared and subsampled to serve as buffer to both sample S5 (VitE-TPGS only) and sample S7 (VitE-TPGS and eltrombopag olamine (PSC)).
b) *Sample S5 (unloaded micelles):* 82.6 mg of vitE-TPGS were solubilized with 19.9 g of the stock pH6.8 (50mM) solution to reach a concentration of 0.41wt%. The sample was stirred for 40 minutes to achieve full dissolution. No significant variation was observed for the pH, in comparison to the stock solution (as expected since VitE-TPGS has no acidity / basicity). The final value measured was pH=6.83. An aliquot of sample was then filtered four times through Axiva sterile cellulose acetate syringe filters with pore diameter of 200 nm. SAXS data collected on the unfiltered and filtered sample were superimposable, indicating that no undissolved surfactant in the form of particulate with size greater than 200 nm was present in the unfiltered sample.
c) *Sample S7 (loaded micelles)*: To 10 g of the S5 solution, eltrombopag olamine powder was added to reach a concentration of 0.08wt% of PSC. The solution was stirred for 60 minutes at 500 rpm. After stirring no significant deviation towards higher pH values was observed thanks to the buffer capacity. The final value measured was pH=6.89. The sample was centrifuged for 2 minutes at 13,000 g and then syringe-filtered as reported for the S5 sample.

All preparations were performed at 25°C.

Table 1 summarizes the physical properties of the chemical compounds used in the experiments. N_A is the Avogadro Number 6.022×10^{23} mol^{-1}. The absolute electron density values $\rho[n_e/Å^3]$ in the 8th column of Table 1 are obtained from the number of electrons per liter n_e/L in column 7th by converting L into Å^3 and making explicit the numerical value of the Avogadro's number N_A. In turn, the n_e/L values in the 7th column are obtained by multiplying the number of moles/L in the 6th column times the number Ne of electrons/molecules as reported in the 4th column times the Avogadro's number N_A. The mass density of alpha-tocopherol[12] PEG[13] and succinate linker[14] were directly taken from the literature.

Monomer volumes for the compounds considered in the study are calculated from published specific densities[15]. TPGS has the following nomenclature Cx=33Fy=22, where x refers to the number of C atoms in the alkyl chain and y to the average number of polyoxyethylene

Table 1
Summary of the physical properties of all chemical compounds used in the experiments. n_e/L number of electrons per liter, N_A is the Avogadro Number.

Compound	Mass Density (g/cm^3)	Mole Mass (g)	N_e= n_e / molecule	Monomer or Molecule Volume (Å^3)	Mole/L	n_e/L	Electron Density ρ n_e /Å^3
vitE-TPGS (n~22-23)	1.08	1499.9-1544.0	820-844	2306-2374	0.720-0.700	590.4-590.8×N_A	0.356
$C_{33}O_5H_{54}(CH_2CH_2O)_n$ n=0.7×22+0.3×23		1513.1	827	2326	0.714	590.5×N_A	0.356
Alpha-tocopherol ($C_{29}H_{50}O_2$)	0.95[a]	430.7	240	753	2.205	529.2×N_A	0.319
TPGS-tocopherol moiety ($C_{29}H_{49}O$)	0.95	413.7	231	723	2.297	530.6×N_A	0.319
TPGS-PEG moiety: PEG-1000 $H(CH_2CH_2O)_n$ **n=0.7×22+0.3×23**	1.20[b]	983.3	536	1360.7	1.220	653.9×N_A	0.394
Succinate Linker ($C_4H_4O_4$)	1.56[c]	116.1	60	123.6	13.44	806.4×N_A	0.486
H_2O	1.00	18.016	10	29.9	55.51	555.1×N_A	0.334
NaOH	2.13	39.997	20	31.2	53.19	1065.1×N_A	0.614
K_2HPO_4	2.44	174.176	86	118.6	14.01	1204.8×N_A	0.726
Stock Solution pH6.8 50 mM	1.01	/	/	/	/	559.6×N_A	0.337
eltrombopag olamine	1.327	564.643 (442.475 as free acid)	232	553.9	2.99	693.7×N_A	0.419

[a] See Ref.6.
[b] See Ref.7.
[c] See Ref.8.

glycol units. The mass density of TPGS is 1.06 g/cm^3 at 50°C and 1.03 at 90°C.[8] Assuming linearity, at room temperature (about 25°C) we expect a mass density of approximately 1.08 g/cm^3. The volumes occupied in solution by the different molecular portions of the surfactant (alpha-tocopherol moiety, succinate linker and PEG chain) were estimated using atomic volume increments[14] or directly reported values available from the literature, in which case Table 1 explicitly reports the literature reference we adopted.

SAXS Measurements

SAXS measurements were performed at SAXSLab Sapienza with a Xeuss 2.0 Q-Xoom system (Xenocs SA, Grenoble, France), equipped with a micro-focus Genix 3D X-ray source with Cu anode (λ = 1.542 Å) and a two-dimensional Pilatus3 R 300K detector which can be placed at variable distance from the sample (Dectris Ltd., Baden, Switzerland). The beam size was defined to be 0.5 mm × 0.5 mm through the two-pinhole collimation system equipped with "scatterless" slits. Calibration of the scattering vector q range [$q=4\pi\sin\theta/\lambda$ with 2θ the scattering angle and λ the photon wavelength], was performed using silver behenate. Measurements with different sample-to-detector distances were performed so that the overall explored q region was 0.01 Å^{-1} < q < 1.5 Å^{-1}, as shown by the experimental SAXS data in Fig. S2 of the Supplementary Material. The lowest accessible q value by our SAXS equipment allows us to register in the SAXS patterns contributions due to scattering of micelles with a maximum size of approximately 60 nm. SAXS contribution from micelle with size above this threshold eventually present in the solution would overlap with the direct X-ray beam and would not be detectable.

Samples were loaded into vacuum-tight quartz capillary cells with thickness 1.5 mm and measured in the instrument sample chamber at reduced pressure (~0.2 mbar) and at room temperature (25±1°C). The two-dimensional scattering patterns were subtracted for the "dark" counts, and then masked, azimuthally averaged, and normalized for transmitted beam intensity, exposure time and subtended solid angle per pixel, using the FOXTROT[16] software developed at SOLEIL synchrotron facility. The one-dimensional intensity vs. q profiles were then subtracted for the solvent and cell contributions and put on absolute scale units (cm^{-1}) by using water as a normalization standard.[17] Precisely, to obtain the scattering profiles shown in Fig. S2, the one-dimensional Intensity vs. q data obtained by azimuthally averaging the 2D patterns and normalization for transmission, acquisition time and subtended solid angle per pixel, have already been subtracted by the corresponding I vs. q data measured for the solvent (aqueous buffer) inserted in the same capillary cell used for measuring the micellar samples. The calibration is based on the assumption that the macroscopic scattering cross-section of pure water is a known value (0.01632 cm^{-1} at 20°C), and the scattering from a sample of pure water is measured in nominally the same capillary cell used to measure the samples.

The different angular ranges were merged using the SAXS utilities tool.[18] Guinier fit analysis and the calculations of Pair Distance Functions (PDF) were performed with the Data Analysis tools of the ATSAS package[19] implementing the GNOM software[20] and using default settings.

Since each lab-SAXS data acquisition lasted approximately one week, the acquisition of individual sets of data has been executed with fresh samples each time prepared before the data acquisition.

The Two-Phase Core-Shell Spherical Theoretical Model

We developed a simple two-dimensional/two-components model that describes the structure and functionality of the VitE-TPGS system micelles assuming a hydrophobic inner core and an outer hydrated hydrophilic shell. Fig. 1 pictorially describes our micelle model system. Through the identification of parameters that are a function of the micelle's size, the fit of the experimental SAXS data against our model returns optimized micelle's size values, under a spherical hypothesis. The mathematical model, whose details are provided in the Supplementary Material, is developed under a more general hypothesis of ellipsoidal micelles, then applied to our experimental data under the simplified spherical assumption, which was suitably fitting the data. The micellar dispersion, at the studied concentration of 0.4 wt% VitE-TPGS, is assumed to be an ideal solution of spherical aggregates in which inter-micellar interference effects are negligible. This assumption is made based on preliminary experimental tests performed at concentrations between 5 and 0.18%wt. The optimum

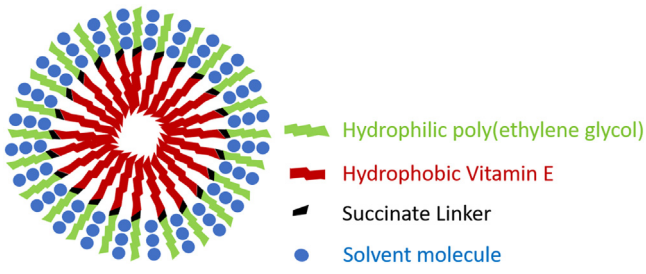

Figure 1. Micelle model system.

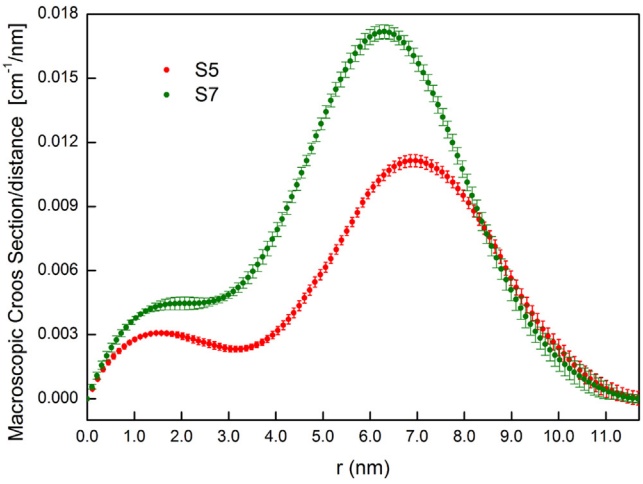

Figure 2. Pair Distance Function PDF(r) of the S5 (unloaded micelles) and S7 (micelles loaded with eltrombopag olamine powder) samples.

value of 0.4%wt was identified as the value corresponding to which no coexistence of large aggregates was observed while still generating a strong enough SAXS signal.

Results and Discussion

SAXS Experimental Results

Fig. 2 shows the Pair Distance Function PDF(r) obtained by indirect Fourier transform of the experimental SAXS data of samples S5 and S7 in the scattering range between 0.09-1.47 nm^{-1} for sample S5 and between 0.12-1.71 nm^{-1} for sample S7. For both S5 and S7 samples, the profiles shown in Fig. 2 are averages of the individual PDF(r) curves obtained from data collected on two independent sample preparations.

The PDF(r) curves describe the SAXS macroscopic cross-section as a function of the atom-atom distances r (in nm). The PDF(r) values, calculated by the software GNOM[20] were multiplied by a factor 4π so that the integral of the PDFs plotted in Fig. 2 is equal to I_0 [cm^{-1}], i.e. the SAXS macroscopic cross-section for the whole sample extrapolated for q=0. For mathematical details see Equations SM15-SM19 in the Supplementary Material.

The I_0 corresponding to sample S7 is appreciably larger than that corresponding to sample S5. Having the two samples the same identical TPGS weight concentration, the larger I_0 value can only be attributed to the incorporation of a fraction of the PSC molecules into the micelles. This experimental semi-quantitative observation made possible by the analysis of SAXS scattered intensity data on an absolute intensity scale, is already *per-se* a relevant result as it suggests an easy experimental tool to semi-quantitatively monitor the drug load and unload in the micelles. With the term semi-quantitative analysis, we refer to a quantitative analysis on a relative scale that allows us to assess whether the micelles in sample A are more or less loaded with drug substance with respect to sample B.

Analytical Modelling of SAXS Data to Extract Quantitative Information of Micelles Size/Shape

Could absolute quantitative information be extracted from the SAXS experimental data? The ability to extract absolute quantitative information would constitute a substantial step forward in the analysis of the VitE-TPGS micelles as we could extract absolute numerical values of relevant structural parameters such as the size of micelles. Assessing the absolute micelles average size under a shape hypothesis is surely stronger than being able to say that micelles in sample A are in the average larger than the micelles in sample B.

Extracting absolute quantitative information from the Pair Distribution function PDF(r) derived from experimental SAXS data, via a fit of experimental data against an analytical theoretical model, is the core purpose of this work.

The general mathematical development that brings to the analytical expressions for PDF(r) functions for two-component ellipsoid-shaped micelles to be fit to the experimental data, is provided in detail in the Supplementary Material section (see Equations SM1-SM14). The model assumes sharp electron density interfaces between the components constituting the micelles that are mathematically modelled via step-like functions. In real micelles, the electron density is expected to have smoother than step-function-like transitions. This smooth transition of the electron density value at the interface between the micelle's components is simulated in our model with a convolution of the analytical model prediction $PDF_{sph}(r)$ based on step-functions with a gaussian function of suitable width σ. The obtained smoothed $PDF_{sph,\sigma}(r)$ function reduces the interference effects of the amplitude scattered by the shells constituting the micelle, to the level consistent with what observed in the experimental data.

Furthermore, to ensure that the smoothed theoretical prediction satisfies the boundary conditions that PDF(r=0)=0 and PDF(r≥D_M)=0, smoothed and unsmoothed PDF functions were combined through a suitable weighting function w(r) while imposing the conditions that PDF(r)=0 both for r=0 and r=D_M (See Equation SM14 in the Supplementary Material section).

A N-shell spherical micelle's model[21] could, in principle, simulate the same smoothing effect on the electron density at the interfaces and therefore describe real profiles. However, this alternative approach would imply the use of a much larger number of free parameters to fit the experimental data than those requested by our analytic model. For a two-components model, our model engages only six parameters: the electron density values for the spherical micelle's hydrophobic core and hydrophilic shell compartments, the electronic density of the aqueous solvent, the core and outer shell sizes and a smoothing parameter (σ). A-priori knowledge of the solvent composition, whose electron density is very close to the water's value, further reduces the free parameters.

For absolute SAXS intensity's data, the model also depends on the number N_{agg} of monomers aggregated to form a micelle, which can be readily derived by fitting the experimental data with the theoretical predictions (see the Supplementary Materials Equations SM23 and SM39). The micellar sizes and electron densities and the N_{agg} are further related to each other by the known atomic composition and the assumed occupied volume. Furthermore, the electron density of the micelle's shell can be expressed as a function of the PEG, succinate and solvent volume fractions, N_{agg} and PEG, succinate and solvent electron densities (see Equations SM15-SM17 in the Supplementary Materials). Thus, for sample S5, N_{agg} can be considered a further free parameter of the model, in place of the shell electron density, to be determined by comparing theoretical and experimental results. For sample S7 which, in principle, could incorporate PSC molecules, the model shall contemplate an additional free parameter, related to the quantity of PSC inside the shell (see Supplementary Materials Equations SM36- SM38).

Instead of fitting the experimental SAXS patterns, the fit of the experimental data against the model is performed in the direct space, which requires the application of an inverse Fourier Transform on the experimental data to move from the reciprocal space of the scattered intensities to the direct space of the atom-atom distances. The inverse Fourier Transform is reliably calculated by the GNOM software. The SAXS patterns in Fig. SM2 are characterized by large errors on smaller spatial scales, but, by definition of Fourier Transform, all

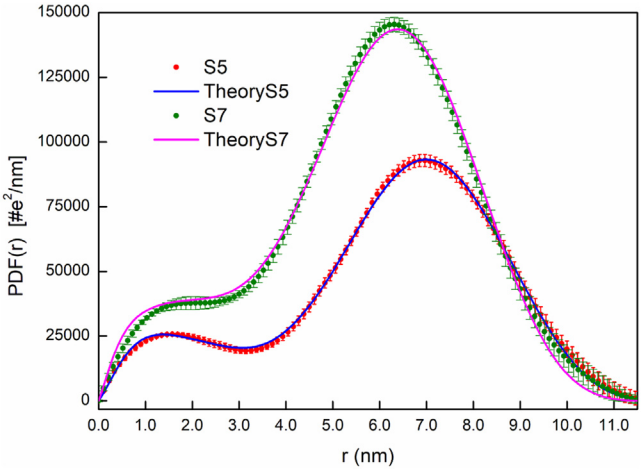

Figure 3. Comparison between experimental PDF(r) and theoretical prediction.

SAXS experimental data contribute to each point of the PDF(r). Hence the overall experimental uncertainties are evenly distributed in PDF (r) curves over the entire r range explored, with larger errors affecting the high q-values balanced by the smaller errors affecting the low q-values. This finding allows a reliable estimate of the micelle size and shape.

Fig. 3 shows the comparison between the experimental PDF(r) obtained on samples S5 and S7 and the prediction of the analytical model, obtained via the algorithm described in the Supplementary Material.

The experimental curves in Fig. 3 have been obtained from the PDF(r) in Fig. 2 by dividing each point by the term K calculated in the Supplementary Materials, (see Equation SM22), which is equal to 1.23×10^{-7} cm^{-1} for both samples S5 and S7. The normalization via the K factor consists of imposing that the integral of the plotted PDF (r) curves be equal to the squared number of excess electrons with respect to the solvent value, per each monomer constituting the micelles and per each distance in nm (see Equations SM36-SM37 in the Supplementary Materials).

The parameters of the micelles' structure obtained through the fits shown in Fig. 3 are schematically represented in Fig. 4 and numerically reported in Table 2, for the investigated samples. ρ_{th}=0.356 el./Å^3 is the nominal density value associate to the compound (see Table 1). σ is the smoothing parameter; N_{agg} is the number of monomers constituting the micelles; std/mean is the ratio of the standard deviation between the theoretical and experimental data, divided by the mean value of the PDF(r). The last column in Table 2 states the ratio between the standard deviation and the mean value for the experimental data.

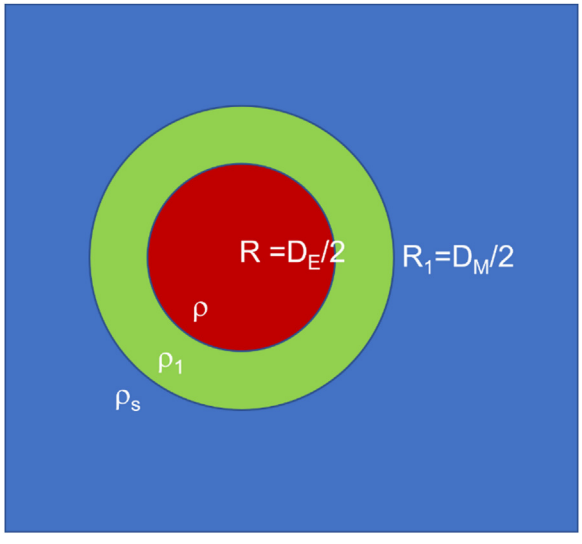

Figure 4. Parameters of the micelles' structure obtained through fits.

In the Supplementary Material we derived an approximate analytical formula (see Equation SM35) to estimate the micelle's core electron density ρ. We obtain: $\rho/\rho_{th} \cong 0.83$ for sample S5 from the maximum distances in the PDF(r) and gyration radius. ρ_{th} denotes the TPGS nominal electron density $\rho = 0.83 \times 0.356 = 0.295$ e/Å^3. The fitting parameters reported in Table 2 have been obtained by minimizing the ratio of the standard deviation between the theoretical and experimental PDF(r) with an algorithm, described in the Supplementary Material, based on the analytical model here discussed. The agreement between the simple theoretical model – a two-component spherical micelle – and experimental data is very good (see Fig. 3), as it can be evinced also from the standard deviation between the theoretical predictions and the experimental data. Therefore, we can conclude that this simplified micelle-structure's model describes efficiently the main structural characteristics of vitE-TPGS micelles, also in the presence of PSC (sample S7).

Table 2 summarizes the physical parameters, characterizing the micelles' structure, as found when fitting the PDF(r) curves extracted from SAXS data. The values of the sample S5's electron densities for the core (ρ = 0.300 ± 0.001 e/Å^3) and the shell (ρ1=0.374 ± 0.001 e/Å^3) should be compared with the values estimated on the basis of densities for the pure alpha-tocopherol, which represent the hydrophobic portion of the VitE-TPGS (ρ =0.319 e/Å^3), and a PEG chain (ρ= 0.394 e/Å^3), as reported in Table 1. The slightly lower value found for the electron density of the core suggests a less dense packing of the vitamin E moiety in the micellar core compared to the molten phase, with a ratio (0.300 ± 0.001)/0.319=0.94 ± 0.003 giving an indication of the volume fraction occupied. This value for the core electron density can be also compared to those reported for the portion occupied by the hydrocarbon methylene groups in lipid bilayers of 0.285 e/Å^3,[22] or in the interior of cationic surfactant micelles of 0.275 e/Å^3.[23] Finally, admitting a core of only aliphatic chains of the alpha-tocopherol (excluding the portion with rings which is denser), the estimate of the electron density based on the volumes of Durchschlag[14] is 0.298 e/Å^3. For sample S7 values about 5% lower than those of sample S5 are obtained, implying a lower packing efficiency of the hydrophobic chains into the internal core, due to the presence of the bounded PSC molecules.

The fit of the experimental data to the theoretical model gives N_{agg}=116±1 for the S5 sample (see Table 2), quite in agreement with works of other authors.[24] This value is compatible with PEG-1000 methyl-terminated surfactants, as shown in the Supplementary Material: see Eq. (S39). The solvent molecules into the hydrated corona, i.e., into the micelle's shell, occupy 42% of the volume. This finding implies that the hydrophilic ends of the VitE-TPGS micelles are quite free of moving. For this reason, in other theoretical approaches the outer shell made of PEG chains has been described as a diffuse corona, described as consisting of non-interacting Gaussian chains, i.e., assuming a mushroom polymer configuration, attached to the compact hydrophobic spherical core.[25] The Gaussian filtering introduced in our modeling takes into account the not compact structure of the interfaces between different blocks constituting the micelles, in particular that between the micelle and the solvent, due to the presence of a diffuse (not compact) hydrated corona. In turn, the large space available into the shell of the micelles constituting sample S5 allows the possibility for other molecules to be incorporated, as investigated for sample S7, in presence of the active pharmaceutical ingredient (PSC molecules).

Table 2
Summary of the parameters values as obtained by fitting the experimental PDF(r) data against the analytical model described in the Supplementary Material. D_M and D_E are the external and internal diameters of the micelle model in Fig. 4; ρ_{th}=0.356 el./Å^3 is the nominal value of electron density for the pure vitE-TPGS compound in the liquid phase (Table 1 of the main text); σ is the smoothing parameter which accounts for not-abrupt electron density interfaces; N_{agg} is the number of monomers aggregated in the micelles; r_{PSC} is the ratio of PSC molecules and Nagg in the micelles.

Sample	D_E [Å]	D_M [Å]	ρ/ρ_{th} ρ [n_e/Å^3]	ρ_1/ρ_{th} ρ_1 [n_e /Å^3] (*)	σ [Å]	N_{agg}	Number of solvent molecules per monomer	r_{PSC}	std/mean between model and exp. Data	std/mean of Exp. Data
S5	58.0 ± 1.0	91.5 ± 0.5	0.844 ± 0.002 0.300 ± 0.001	1.051 ± 0.002 0.374 ± 0.001	28 ± 0.5	116 ± 1	36 ± 1	0	0.025	0.055
S7	50.0 ± 1.0	87.5 ± 0.5	0.792 ± 0.002 0.282 ± 0.001	1.073 ± 0.002 0.382 ± 0.001	29 ± 0.5	117 ± 1	26 ± 1	0.30 ± 0.01	0.047	0.045

(*) This quantity is not a free parameter of the fitting procedure, but for sample S5 it is obtained using Equation SM15 of the Supplementary Material, as a function of D_E, D_M and N_{agg} values determined by the fit and based on the molecular volumes reported in Table 1. For sample S7, ρ_1/ρ_{th} also depends on $r_{PSC,}$ i.e, the ratio of PSC molecules and N_{agg} inside the micelles per each monomer incorporated into the micelles (see Equation SM17 of the Supplementary Material.

Incorporation of the PSC Molecules into the vitE-TPGS Micelles

We would like to estimate how much of the PSC in solution has been efficiently incorporated into the vitE-TPGS micelles. In the Supplementary Material (Eqs. SM36-SM38) we have estimated, based on the sample composition and experimental SAXS data, that the maximum ratio of PSC molecules per VitE-TPGS monomer inside the micelles is $(r_{PSC})_{max}$=78/117∼2/3. With a higher concentration of PSC molecules in the initial solution one might expect the ideal value of $(r_{PSC})_{max}$=1, i.e. one PSC molecule per vitE-TPGS micelle, to be accessible. The best fit of our model to the experimental data returned r_{PSC} 0.30±0.01 (see Table 3). This means that only less than one half of the available PSC molecules in solutions has been incorporated into the TPGS micelles due to affinity competition with the media vs micelles. Understanding the partition coefficient between the micelle and the media is very insightful and is likely to be translated into bioavailability. Where are located the active pharmaceutical moieties effectively incorporated into the micelle? To answer this question, in Fig. 5 we performed a fit with a three-spherical shell model (blue curve) of the experimental difference (red points) between the PDF (r) of sample S7 (loaded micelles) and the PDF(r) of sample S5 (unloaded micelles). The size of loaded and unloaded micelles is different. Therefore, the difference of their PDFs could give negative values. In other words, the need to insert a second shell is due to the presence of negative values of the $PDF_{S7}(r) - PDF_{S5}(r)$ difference, in turn, related to the different size of the S7 and S5 micelles. The equations for the three-spherical shell model are derived in the Supplementary Material (Equations SM40-SM47; Fig. SM3).

In the fit some quantities are kept fixed, namely N_{agg}=117 and r_{PSC}=0.3. The numerical results for the best fit (blue curve of Fig. 5) are reported in Table 3. We have 6 free parameters: the core size, the two shell sizes (D_M-2t and D_M), where t is the thickness of the outer shell; the core and the outer-shell electron densities (ρ and ρ_C), the smoothing parameter σ. For the intermediate shell, between the core and the outer shell, we have that the electron density value ρ_1 is obtained using Equations SM16 and SM17 in the Supplementary Material. Therefore, it is not a free parameter since we fixed r_{PSC}=0.3, obtained by the previous fit of S7 data. Indeed, ρ_1 is function of quantities already determined by the other two fits. Nevertheless, we found a good agreement between theory and experimental data, confirming that the PDF differences between S7 and S5 samples are effectively due to the incorporation of PSC molecules. Both for the core and the outer shell, we found small negative electron density values, implying that, in the corresponding regions of the micelles, the S7 sample values are slightly smaller than the S5 sample values (see the minus sign in Table 3). We interpret these local negative electron density values as an indication that the presence of the incorporated PSC molecules causes small structural changes to the original vitE-TPGS micelle structure. Indeed, the size reduction is not only a mere volume effect. The PSC molecules replace some of the solvent molecules, as clearly evidenced by the change in the number of solvent molecules per monomer from 36 (S5) to 26 (S7), as reported in Table 2. Therefore, a colocalization of PCS molecules and hydrophilic head of the VitE-TPGS carrier can be inferred.

As shown by the last two columns of Table 3, the std/mean ratio between the model and the experimental data is smaller than the experimental std/mean ratio, assessing the reliability of the fit. It should be observed that the electron density values in the core as predicted by the model are systematically larger than the experimental values, both in Figs. 3 and 4. Close to the origin the agreement between the theory and the experimental data is slightly worse for loaded micelles (sample S7) with respect to unloaded micelles (sample S5) (see Fig. 4). This finding can be related to the assumption in our simplified model of a constant electron density into the core. In real micelles we should expect an electron density which is smaller close to the origin (r=0) and increases going towards the core surface, due to the reduction of space allowed for packing hydrophobic chains in the inner regions of the micelles. This finding causes the slight overestimation of the theoretical PDF(r) values with respect to real values, in the inner regions of the micelles, due to the simplified model here assumed, with a constant electron density everywhere in the core. This overestimation is larger for the loaded micelles.

Table 3
Values of the parameters obtained by the fit of the experimental $PDF_{S7}(r) - PDF_{S5}(r)$ data with the analytical model described in the Supplementary Material. Here the free parameters are: the core size (D_E); the thickness of the outer shell (t); the two shell sizes (D_M-2t and D_M), the core and the outer-shell electron densities (ρ and ρ_C), the smoothing parameter (σ).

PDF Difference	D_E [Å]	D_M-2t [Å]	D_M [Å]	$-\rho$ [e/Å^3]	ρ_1 [e/Å^3]	$-\rho_C$ [e/Å^3]	σ [Å]	std/mean* between model and exp. data	std/mean** of Exp. Data
S7-S5	58.0 ± 1.0	74.0 ± 1.0	101.0 ± 1.0	0.019 ± 0.001	0.073 ± 0.001	0.002 ± 0.0001	22.5 ± 0.5	0.13	0.182

* *std/mean* is the ratio of the standard deviation between the theoretical and experimental data, divided by the mean value of the $PDF_{S7}(r) - PDF_{S5}(r)$
** *std/mean* is the ratio between the experimental standard deviation and the mean value for the $PDF_{S7}(r) - PDF_{S5}(r)$ experimental data

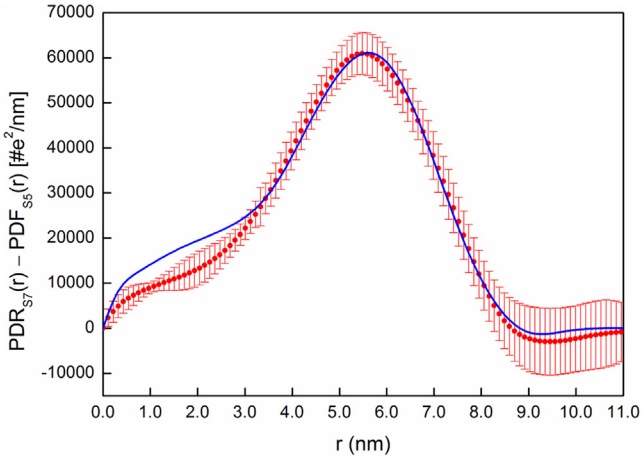

Figure 5. Fit with a three-spherical shell model (blue curve) of the experimental difference (red points) between the PDF(r) of sample S7 (loaded micelles) and the PDF(r) of sample S5 (unloaded micelles).

Finally, we obtain that (D_M-2t- D_E)/2=8.0 Å. This is the size of the first shell region, starting from the linker succinate, where the presence of the PSC molecules is concentrated.

Conclusions

The incorporation of PSC, here exemplified by eltrombopag, within the VitE-TPGS micelles produces an evident modification of the SAXS profile, signifying both a decrease of the correlation atom-atom distances and an increase of the shell electron density, due to the extra electrons incorporated. According to the two-phase core-shell spherical model we developed, the observed experimental changes are interpreted as a reduction of the hydrophobic core radius and a decrease of their associated electron density. Conversely, the shell simultaneously increases in both volume and electron density. At a molecular level, this observation suggests a preferential localization of the PSC molecules close to the intermediate portion of the vitE-TPGS molecule represented by the succinate linker and the benzodihydropyran rings, which link the more markedly hydrophobic aliphatic chains of the alpha-tocopherol moiety and the hydrophilic PEG chains. In the absence of the loaded pharmaceutical active ingredient, the model would include within the core the whole alpha-tocopherol moiety, whereas the addition of the PSC molecule would produce a shrinkage of the less electron dense internal core in favor of a more electron dense shell. The approach can also open new perspectives as a tool to directly determine the partition coefficient of a PCS between solution and within the supramolecular assembly without further manipulation of the solution, or as experimental description to define a starting point for further modeling and simulation, that might be used to optimize and retro-engineer enhanced properties.

Declaration of Interests

The authors declare that they have no known competing financial interests or personal relationships that could have appeared to influence the work reported in this paper.

Acknowledgments

The Sapienza Research Infrastructure is acknowledged for the SAXS measurements at SAXSLab Sapienza, funded by the Large Equipment Project 2015-C26J15BX54.

Supplementary Materials

Supplementary material associated with this article can be found in the online version at doi:10.1016/j.xphs.2022.09.029.

References

1. Ahmed TA, El-Say KM, Ahmed OAA, Aljaeid BM. Superiority of TPGS-loaded micelles in the brain delivery of vinpocetine via administration of thermosensitive intranasal gel. *Int J Nanomedicine*. 2019;14:5555–5567.
2. Limongi T, Susa F, Marini M, et al. Lipid-based nanovescicular drug delivery systems. *Nanomaterials*. 2021;11(12):3391.
3. Svergun DI, Shtykova EV, Volkov VV, Feigin LA. Small-angle X-ray scattering, synchrotron radiation, and the structure of bio- and nanosystems. *Crystallogr Rep*. 2011;56(5):725–750.
4. Guinier A, Fournet G. *Small-Angle Scattering of X-Rays*. New York: John Wiley; 1955.
5. Glatter O, Kratky O. *Small-angle X-ray scattering*. Academic Press; 1982.
6. Svergun DI, Koch M H J. Small-angle scattering studies of biological macromolecules in solution. *Rep Prog Phys*. 2003;66:1735.
7. Guo Y, Luo J, Tan S, Otieno BO, Zhang Z. The applications of vitamin E TPGS in drug delivery. *Eur J Pharm Sci*. 2013;49(2):175–186.
8. Papas MA. Vitamin E TPGS and its applications in nutraceuticals. In: Gupta, Lall, Srivastava, eds. *Nutraceuticals - Efficacy, Safety and Toxicity*. 2nd ed. Elsevier Inc., Academic Press; 2021:991–1010. 2021.
9. Drug approval package: promacta (Eltrombopag) NDA#022291.
10. Opinion of the Scientific Panel on Food Additives, Flavorings. Processing aids and materials in contact with food on a request from the commission related to d-alpha-tocopheryl polyethylene glycol 1000 succinate (TPGS) in use for food for particular nutritional purposes. *Eur Food Safety Authority (EFSA) J*. 2007;490:1–20.
11. Kaduk J, Gindhart A, Blanton T. Crystal structure of eltrombopag olamine form I, (C2H8NO)2 (C25H20N4O4). *Powder Diffr*. 2021;36(2):100–106. https://doi.org/10.1017/S0885715621000099.
12. Niki E, Abe K. Vitamin E: structure, properties and functions. In: Niki E eds. Vitamin E: Chemistry and Nutritional Benefits, Royal Society of Chemistry, 2019 (Chapter 1):1–11.
13. Sommer C, Pedersen JS, Stein PC. Apparent specific volume measurements of poly (ethylene oxide), poly(butylene oxide), poly(propylene oxide), and octadecyl chains in the micellar state as a function of temperature. *J Phys Chem B*. 2004;108:6242–6249.
14. Durchschlag H, Zipper P. Calculation of the partial volume of organic compounds and polymers. In: Lechner MD, eds. Ultracentrifugation. Progress in Colloid & Polymer Science, vol. 94; 1994: 20-39.
15. le Maire M, Champeil P, Moller JV. *Biochim Biophys Acta*. 2000;1508(1-2):86–111.
16. https://support.foxtrotalliance.com/hc/en-us/articles/115003492045-Setup-Instructions-Install-and-set-up-Foxtrot-FoxHub-and-FoxBots.
17. Orthaber D, Bergmann A, Glatter O. SAXS experiments on absolute scale with Kratky systems using water as a secondary standard. *J Appl Crystallogr*. 2000;33:218–225.
18. Sztucki M, Narayanan T. Development of an ultra-small-angle X-ray scattering instrument for probing the microstructure and the dynamics of soft matter. *J Appl Crystallogr*. 2007;40:s459–s462.
19. Manalastas-Cantos K, Konarev PV, Hajizadeh NR, et al. ATSAS 3.0 : expanded functionality and new tools for small-angle scattering data analysis. *J Appl Crystallogr*. 2021;54:343–355.
20. Svergun DI. Determination of the regularization parameter in indirect-transform methods using perceptual criteria. *J Appl Crystallogr*. 1992;25:495–503.
21. Ivanović MT, Hermann MR, Wójcik M, Pérez J, Hub JS. SAXS curves of detergent micelles: effects of asymmetry, shape fluctuations, disorder, and atomic details. *Phys Chem Lett*. 2020;11(3):945–951.
22. Heftberger P, Kollmitzer B, Heberle FA, et al. Global small-angle X-ray scattering data analysis for multilamellar vesicles: the evolution of the scattering density profile model. *J Appl Crystallogr*. 2014;47:173–180.
23. Schmutzler T, Schindler T, Schmiele M, et al. The influence of n-hexanol on the morphology and composition of CTAB micelles. *Colloids Surf A Physicochem Eng Asp*. 2018;543:56–63.
24. Puig-Rigall J, Grillo I, Dreiss CA, González-Gaitano G. Structural and spectroscopic characterization of TPGS micelles: disruptive role of cyclodextrins and kinetic pathways. *Langmuir: ACS J Surf Colloids*. 2017;33(19):4737–4747.
25. Pedersen JS. Form factors of block copolymer micelles with spherical, ellipsoidal and cylindrical cores. *J Appl Cryst*. 2000;33:637–640.